ASM Handbook, Volume 11, *Failure Analysis and Prevention*
B. Miller, R. Shipley, R. Parrington, D. Dennies, editors
DOI 10.31399/asm.hb.v11.a0006795

Erosive Wear Failures

Revised by Maksim Antonov, Tallinn University of Technology

EROSION is the progressive loss of original material from a solid surface due to mechanical interaction between that surface and a fluid, a multicomponent fluid, an impinging liquid, or impinging solid particles (Ref 1). Erosion is a rather broad term and can be further classified into more specific terms, including cavitation erosion, liquid impingement erosion, and solid particle erosion. Cavitation erosion is due to the formation and collapse, within a liquid, of cavities or bubbles that contain vapor or gas or both. Liquid impingement erosion is due to impacts by liquid drops or jets. Solid impingement erosion is due to impacts by solid particles. Impingement also connotes that the particles are smaller than the solid surface and that the impacts are distributed over that surface or a portion of it. Erosion can occur in combination with other forms of surface degradation, such as corrosion. This is referred to as erosion-corrosion.

The detrimental effects of erosion have caused problems in a number of industries. In the power-generation industry, erosion damage has occurred to boiler tubes and waterwalls (Ref 2–16), steam turbines (Ref 17–19), land-based gas turbines (Ref 20–22), solids-transport systems (Ref 16, 23–27), cyclones (Ref 16, 27–29), valves (Ref 16, 30, 31), and inlet nozzles (Ref 32). In the oil and gas industry, choke valves are damaged by erosion (Ref 33–36). In the petrochemical industry, process control valves (Ref 36) and power-recovery turbines (Ref 17, 37) are damaged by erosion. In chemical process industries, solids-transport systems are damaged by erosion (Ref 24, 38–40). In the aircraft industry, damage has occurred to aircraft engines (Ref 18, 20, 41–43). The devices for generation of renewable energy (solar panels, turbines of hydroelectric power stations, windmill blades, etc.) also suffer from erosion (Ref 44–46).

Erosion occurs as the result of several different mechanisms, depending on the composition, size, and shape of the eroding particles; their velocity and angle of impact; and composition and properties of the surface material being eroded. The sensitivity of elastic, brittle, and ductile materials to the angle of impact generally follows the behavior shown in Fig. 1, with ductile materials experiencing the maximum rate at approximately 20 to 30° and brittle materials at approximately 90° (Ref 50). This tendency of maximum erosion for a ductile material at approximately 20 to 30° is not universally observed and is dependent on factors such as particle shape and fragmentation (Ref 51–53). When ductile materials are impacted by spherical particles that do not fragment, the maximum erosion rate can occur at 90°, illustrating that material behavior depends on conditions. Elastic materials (e.g., rubber) usually experience the maximum rate at angles lower than for ductile ones (Ref 47, 48), while materials consisting of several phases experience mixed behavior, and their maximum is usually positioned between the maxima of constituents (Fig. 1). The graph of mixed behavior was created based on results (rounded silica sand of 0.1 to 0.3 mm, or 0.004 to 0.01 in., diameter; 61 m/s, or 200 ft/s, velocity) obtained for WC-15wt% Co cemented carbide consisting of brittle tungsten carbide grains and ductile cobalt matrix (Ref 49). Erosion of a given material as a function of time often follows a pattern consisting of an incubation period with little or no material removal, followed by an increasing rate, and finally a steady state. Some materials exhibit peaks with decelerating rate with or without a final steady state (Fig. 2). Most mechanistic models are concerned only with the steady state.

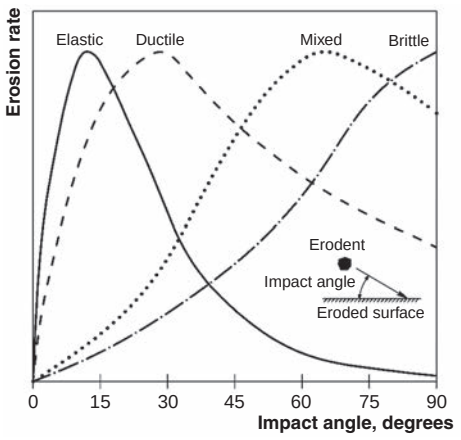

Fig. 1 Relative effect of impact angle on solid particle erosion of various types of materials. The scale for erosion rate is not the same for the different materials. Adapted from Ref 47–49

The surface of material attacked during erosion (tribolayer) differs chemically and physically from the original material. During the incubation period, transformation from original into the characteristic (for given erosive conditions) material surface occurs, including removal of chemicals (e.g., lubricants and cutting fluids remaining after production), a change of topography (removal of grinding marks, etc.), removal of fragments weakened or damaged during the production stage, generation of defects (cracks, etc.), embedment of erodent particles or their fragments (as well as oxide layers, for example) into the surface layer, and possible formation of a mechanically mixed layer (Ref 55). The hardness of the tribolayer of ductile metals (during impingement with a high angle of impact when embedment is favored) can approach that of the erodent particles, which leads to a reduction of the erosion rate. As a result, the behavior of a tribolayer can change from ductile to mixed.

Erosion of materials is attributed to several mechanisms, including cutting (Ref 50, 56–60), fragmentation (Ref 61), elastic and elastic-plastic fracture (Ref 62–64), extrusion (Ref 65, 66), fatigue (Ref 67, 68), delamination (Ref 69, 70), deformation localization (Ref 52, 60, 71, 72), and melting (Ref 43, 65, 71). An even greater number of analytical models have been proposed (Ref 73, 74), but none have been completely satisfactory, especially for multiple-particle impact. A generic, empirical formula for erosion (Ref 5, 35, 36) is a good place to start to show the general trends in modeling erosion, proceeding later to more specific models:

$$E = K_0 V^p f(\alpha) \quad \text{(Eq 1)}$$

where E is the specific erosion rate, V is the particle velocity, p is the velocity exponent, f is a function of the impact angle of the particles (α), and K_0 is a constant that includes all other effects. The velocity exponent, p, varies from 2 to 3 with a mean of approximately 2.4 for ductile materials (Ref 72, 75), while it varies from 2 to 6 with a mean value of approximately 3 for brittle materials (Ref 62, 76, 77). The exponent may vary between different

velocity ranges if the erosion mechanism is changing (thresholds). For example, this can be associated with transfer from high-cycle to low-cycle fatigue or direct removal of material fragments due to increasing impact energy (velocity) of attacking particles or fracturing of the erodent particles after some threshold velocity. It is easiest to consider the erosion of ductile and brittle materials separately, but it must be understood that, in reality, there is a continuum of materials. In addition, some materials, such as composites and cermets, can have both brittle and ductile components and exhibit mixed behavior (Fig. 1).

Erosion of Ductile Materials

The erosion of ductile materials by solid particles can be separated into two components, a cutting component and a deformation component, based on the angle of impact of the particles. The component of the particle velocity parallel to the surface produces the cutting component of erosion. Erosion by cutting is similar to chip formation in machining, in that pieces of material are removed by the impact of a sharp-edged particle. This component dominates the erosion rate at low impact angles. A model for the cutting component was introduced by Finnie (Ref 56–58) and was developed by Bitter (Ref 50) and Neilson and Gilchrist (Ref 59):

$$f_c(\alpha) = A \cos^2\alpha \sin n\alpha \qquad \text{(Eq 2)}$$

where n is $\pi/2\alpha_0$ for $\alpha < \alpha_0$, n is $\pi/2\alpha$ for $\alpha > \alpha_0$, and α_0 and A are constants. This function is illustrated in Fig. 3. The model originally developed by Finnie overestimated the erosion rate, due to material piling up on the sides of the impact site instead of the groove being totally removed as wear debris (Ref 78, 79). However, the model does correctly account for the shape of the erosion curve as a function of impact angle.

The other component of erosion is produced by the component of velocity perpendicular to the surface. Bitter called the component deformation wear (Ref 50). This component involves repeated battering of the surface, leading to the eventual fracture and removal of wear debris (Ref 79). This component was modeled by Bitter (Ref 50) and was developed by Neilson and Gilchrist (Ref 59):

$$f_d(\alpha) = B \sin^2\alpha \qquad \text{(Eq 3)}$$

where B is a constant. This component has the shape of the brittle behavior in Fig. 1. Many mechanisms have been suggested for the deformation component, including an extrusion mechanism with subsequent lip removal (Ref 65, 66), a low-cycle fatigue mechanism (Ref 67, 68), a delamination mechanism (Ref 69, 70), a localization of plastic deformation mechanism (Ref 52, 72), a work hardening with embrittlement mechanism (Ref 50), and a mechanism involving melting (Ref 43). Of these, most studies favor an extrusion with subsequent lip formation, delamination, low-cycle fatigue, or localization of plastic deformation mechanism. Combining the two components leads to the complete angular term:

$$f(\alpha) = A \cos^2\alpha \sin n\alpha + B \sin^2\alpha \qquad \text{(Eq 4)}$$

Particle shape plays a significant role in erosion. Angular particles produce much larger erosion rates than spherical particles, especially at low impact angles (Ref 51–53, 80–83). The change in erosion rate due to particle shape depends mostly on the cutting component (although the particle shape appears to play a role in the deformation component also (Ref 52). Spherical particles produce little or no cutting wear, instead of plowing, which results in $B > A$ in Eq 4. The appearance of a surface eroded by spherical particles is shown in Fig. 4. The surface shows the extruded lip formation or platelet mechanism of the deformation component of erosion. Angular particles usually produce large quantities of cutting wear, which results in $A > B$ in Eq 4. The appearance of a surface eroded by angular particles is shown in Fig. 5. The surface shows the cutting mechanism of erosion. The role of particle shape on the erosion rate has been illustrated a number of times, but it is difficult to quantify, except empirically, because it depends on a large number of properties of both the eroding particle and the surface being eroded (Ref 3–5, 22, 32, 35, 59, 83).

The constant K_0 in Eq 1 includes the effects of several other factors, such as the size of the impacting particles, the hardness of the particles

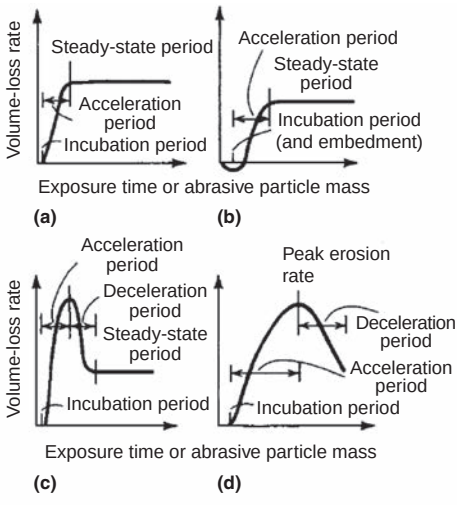

Fig. 2 Characteristic volume-loss rate versus time curves. (a) Type I. (b) Type II. (c) Type III. (d) Type IV. Source: Ref 54

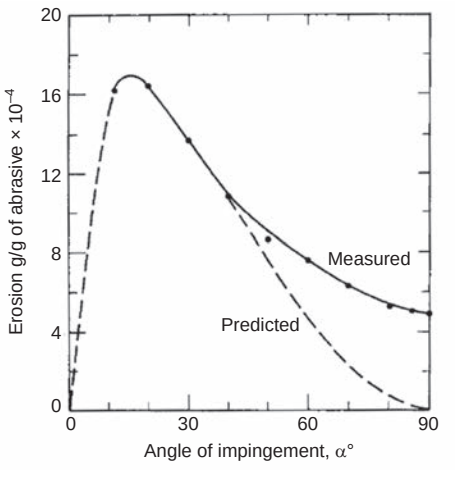

Fig. 3 Experimental and predicted curves of erosion of aluminum by 120-mesh silicon carbide (SiC) particles at a velocity of 152 m/s (500 ft/s). Source: Ref 8

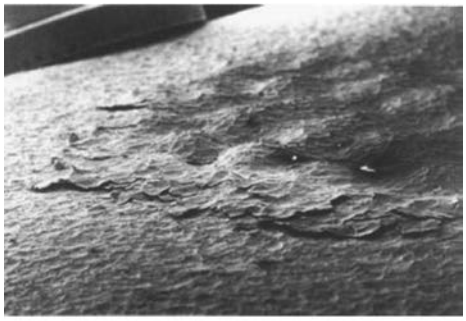

Fig. 4 Surface of 1100-O aluminum (annealed condition) eroded by 700 μm diameter spherical steel shot at 60° impact angle. Source: Ref 8

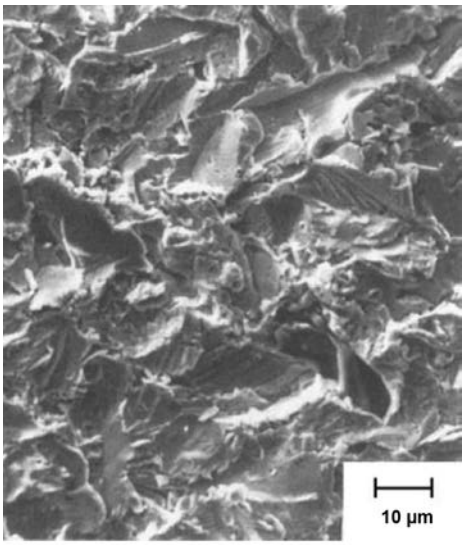

Fig. 5 Surface of AISI 1020 carbon steel eroded by SiC at 80 m/s (260 ft/s) and 30° impact angle. Source: Ref 8

relative to the hardness of the eroded surface, and temperature effects. The first of these factors is the size of the particles (Ref 61, 80, 84). For very small particles (<5 μm), there is no measurable erosion. The erosion rate increases with increasing particle size until an upper limit is reached. Above the upper limit, erosion rate is independent of particle size. This upper limit is approximately 50 to 100 μm. The particle size factor, K_s, can be modeled as (Ref 61):

$$K_s = \left[1 - \left(\frac{d_0}{d}\right)^{3/2}\left(\frac{V_0}{V}\right)\right]^2 \quad \text{(Eq 5)}$$

where d is the particle size, V is the velocity, and d_0 and V_0 are constants.

The second factor is the hardness of the particles relative to the hardness of the surface (Ref 8, 81, 83). This factor is shown in Fig. 6. When particles are more than twice as hard as the surface, the erosion rate is independent of the particle hardness. When particles are less than half the hardness of the surface, erosion is not measurable. Between these limits, there is a continuous transition. This factor, K_h, has been modeled as (Ref 83):

$$K_h = 1 - \exp\left[-\ln 2\left(\frac{H_p}{mH}\right)^{1-2m}\right] \quad \text{(Eq 6)}$$

where H_p is the hardness of the particle, H is the hardness of the surface, and m is a constant.

Increasing the temperature has a mixed effect on the erosion rate for ductile materials (Ref 77, 85). A substantial amount of high-temperature erosion testing has been performed in support of the gas turbine and coal gasification industries. The testing provided a substantial amount of results on temperature effects.

Corrosion can increase or decrease the apparent erosion rate, depending on the rate of oxide or other corrosion product formation and the resistance of the product to erosion compared with the normal surface material (Ref 77, 85). If the corrosion product is slow growing and more erosion resistant than the underlying metal, it can effectively protect the metal from erosion. Similarly, deposition of some process material on the surface can also protect it. These protective mechanisms have been observed on some boiler heat-exchanger tubes, but they are probably more the exception than the rule. More often, oxidation of the underlying metal with rapid removal of the fragile, brittle oxide (particularly at high angles of impact) accelerates erosion.

The three factors—particle size, particle hardness, and temperature (K_t)—can be combined as a product:

$$K_0 = K_s K_h K_t \quad \text{(Eq 7)}$$

Any additional factors, such as fragmentation of the particles, could also be included in Eq 7.

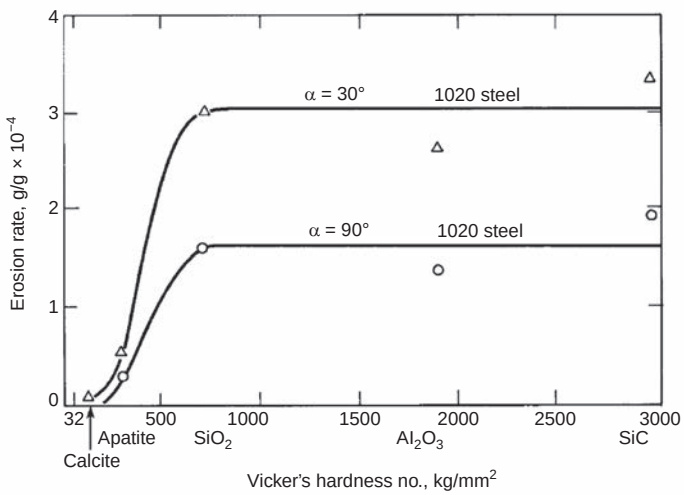

Fig. 6 Erosion rates of AISI 1020 carbon steel by 180 to 250 μm (7 to 10 mils) particles at 80 m/s (260 ft/s)

Erosion of Brittle Materials

Erosion of brittle materials by hard, solid particles involves a process in which material is lost from the target by brittle fracture (Ref 26, 62–64, 76). The size and shape of the cracks that form in the surface depend on several factors, including particle shape, mass, and velocity as well as target material hardness and toughness. The erosion rate correlates with the fracture toughness and hardness given by (Ref 62):

$$E = K_2 V^p R^a \rho^b K_c^c H^d f(\alpha) \quad \text{(Eq 8)}$$

where V is the velocity, R is the particle radius, ρ is the particle density, K_c is the surface material fracture toughness, H is the surface material hardness, and p, a, b, c, d, and K_2 are constants. A regression analysis found the following for the exponents: $p = 2.8$, $a = 3.9$, $b = 1.4$, $c = -1.9$, and $d = 0.48$.

This indicates that the erosion rate increases with increasing hardness of the surface material and with decreasing fracture toughness of the surface material. These exponents were compared to theoretical models based on elastic-plastic fracture (Ref 63, 64), and rough agreement was found (Ref 62). The variation of erosion as a function of impact angle for brittle materials is shown in Fig. 1. Equation 3 can be used to model this curve (Ref 50, 63).

Erosion of Elastomers

The erosion of unfilled elastomers by hard, rounded solid particles is mainly driven by a fatigue mechanism, while erodent particles or their fragments attached or embedded in the material surface can also influence (Ref 86, 87). During erosion, surface irregularities form, tears or networks of cracks are created, and material is lost at their intersections. The shape of surface irregularities depends on elastomer properties. At low angles of impact, ridges or waves accompanied by subsurface tears may be formed on the surface of rubbers with high rebound resilience (Ref 86, 87). The maximum erosion rate of elastomers is usually observed at angles lower than 20° (Fig. 1), and the erosion rate is higher for angular and/or larger erodents (Ref 86). Elastomers with high erosion resistance usually have low modulus (unfilled), high rebound resilience, good fatigue resistance, low coefficient of friction against the erodent particle (to reduce tearing that is significant mostly during impact with low angle of impact), and good resistance to environmental degradation (more significant during erosion with low flux rate) (Ref 86, 88, 89).

Examples of Erosive Wear Failures

Erosive wear occurs in many situations where a large number of small solid or liquid particles impact against a surface or where the collapse of gas-filled bubbles in a cavitating liquid causes surface damage. Some examples of erosive wear failures are given in the following sections on abrasive erosion, liquid impingement erosion, cavitation, and erosion-corrosion. Further discussion can be found in the articles "Abrasive Wear Failures," "Corrosive Wear Failures," and "Liquid Droplet Impingement Erosion" in this Volume.

Abrasive Erosion

The term *abrasive erosion* is sometimes used to describe erosion in which the solid particles move nearly parallel to the solid surface. For example, abrasive erosion in pump components generally occurs due to the impingement of particles at very oblique angles to the surface. Such abrasion attacks ductile materials

much more readily than it does hard, relatively brittle materials, as pointed out by Finnie (Ref 90). Particulate erosion of a ductile steel impeller by a catalytic fluid that was not expected to be erosive is shown in Fig. 7.

Erosion-resistant metals include white cast iron (standard gray or ductile cast irons have poor resistance), high-chromium (that is, 13 to 28%) alloy steel, cobalt-base superalloys such as Stellite, and special nickel-base alloys such as Ni-Hard. These materials are useful not only for the flow-path surfaces but also as sleeves in sealing areas, particularly if packing is used. It is good practice to use hard metal or ceramic expellers near seal entrances to keep particles out of the sealing clearance. If thorough flushing of packing presents a design problem, abrasion-resistant SiC ceramic mechanical seals together with an expeller or minimal flushing can be used. Some of the advanced designs of mechanical seals for abrasive service are even axially split for ease of replacement.

Another example of abrasive erosion is the impact of fly ash entrained in the flue gases in screen tubes or superheater tubes of boiler systems (Ref 91). Erosion is enhanced by high flow velocities; thus, partial fouling of gas passages in tube bands by deposition of fly ash can lead to erosion by forcing the flue gases to flow through smaller passages at higher velocity. This effect, sometimes called laning, exposes tube surfaces to a greater probability of impact by particles having higher kinetic energy, thus increasing the rate of damage. Erosion by fly ash causes polishing, flat spots, wall thinning, and eventual tube rupture. Fly ash erosion can be controlled by coating tube surfaces with refractory cements and other hard, erosion-resistant materials, although this reduces the heat-transfer capability of the surface. An alternative method is the use of baffles to channel gas flow away from critical areas.

Liquid Impingement Erosion

Erosion can occur in a liquid medium even without the presence of solid abrasive particles in that medium (Ref 92). Liquid droplets impacting a solid surface at high speed is the form of liquid erosion called liquid impingement erosion or liquid impact erosion, as discussed in more detail in the article "Liquid Droplet Impingement Erosion" in this Volume and in the article "Liquid Impingement Erosion" in *Friction, Lubrication, and Wear Technology*, Volume 18 of *ASM Handbook*, 2017. Corrosion may or may not occur simultaneously with liquid impingement erosion.

A simplified schematic of liquid impingement erosion processes is illustrated in Fig. 8. The impact-pressure history (and resulting stress waves) can produce circumferential cracks or deformation patterns around the initial area of impact (Fig. 8a), depending on the properties of the surface material and the energy of the impact. Following impact, the liquid flows away radially at high velocity. The spreading liquid can hit nearby surface asperities and the surface steps resulting from plastic deformation caused by the initial impact pressure. The force of this impact stresses the asperity or surface step at its base and can produce a crack (Fig. 8b). Subsequent impacts by other drops can widen the crack or detach a particle entirely (Fig. 8c). Direct hits on existing cracks, pits, and other deep depressions can produce accelerated damage by a microjet impingement mechanism (Fig. 8d). Eventually, the pits and secondary cracks intersect, and larger pieces of the surface become detached.

Among the components most susceptible to liquid impingement erosion are low-pressure turbine blades, low-temperature steam piping, and condenser and other heat-exchanger tubes that are subjected to direct impingement by wet steam. Liquid impingement erosion in tubing and piping is most likely when fluid velocities exceed 2.1 m/s (7 ft/s). Damage occurs first at locations where direction of flow changes, such as elbows or U-bends. Large-radius bends are less susceptible to such damage. However, use of erosion-resistant materials, such as austenitic stainless steel, is often more effective. Erosion of heat-exchanger

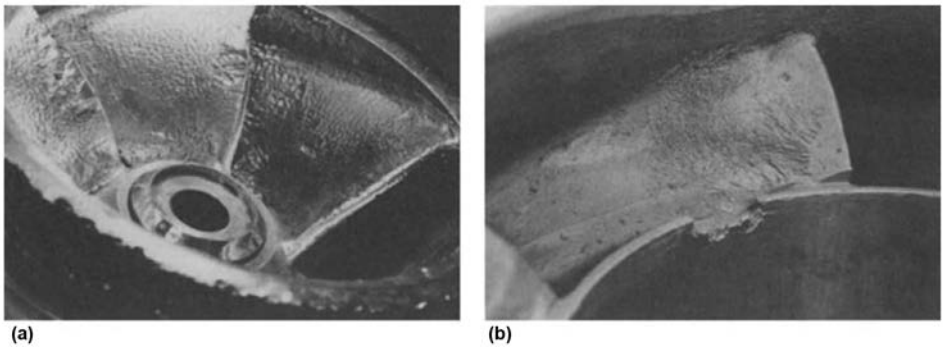

Fig. 7 Particulate erosion of a ductile steel impeller by an abrasive catalyst. Original magnification: (a) 0.25×, (b) 1×

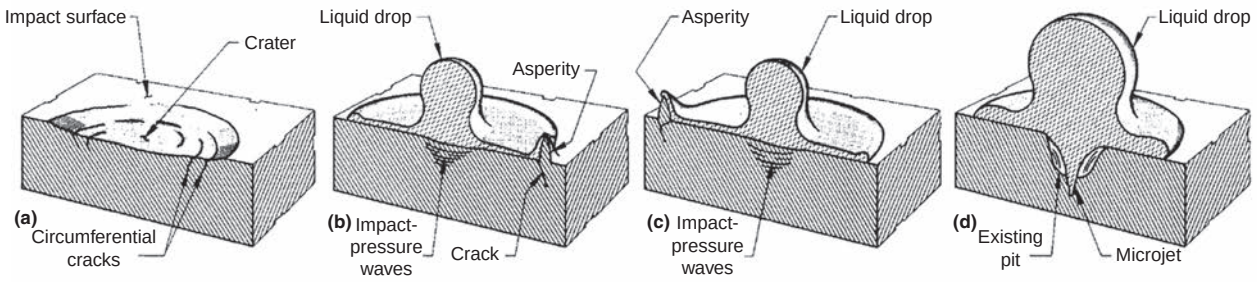

Fig. 8 Processes by which a material is damaged by liquid impingement erosion. (a) Solid surface showing initial impact of a drop of liquid that produces circumferential cracks in the area of impact or produces shallow craters in very ductile materials. (b) High-velocity radial flow of liquid away from the impact area is arrested by a nearby surface asperity, which cracks at its base. (c) Subsequent impact by another drop of liquid breaks the asperity. (d) Direct hit on a deep pit results in accelerated damage, because shock waves bouncing off the sides of the pit cause the formation of a high-energy microjet within the pit.

tubes caused by impingement of wet steam can sometimes be eliminated by redirecting flow with baffles.

Moisture erosion of low-pressure blades has been a problem throughout steam turbine history and remains a concern today. For example, Fig. 9 shows two portions of the leading edge of a blade from the last stage of a low-pressure steam turbine. Liquid impingement erosion in its advanced stages is often characterized by a surface that appears jagged and composed of sharp peaks and pits. One portion (at left, Fig. 9) was protected by an erosion shield of Stellite 6B; the other portion (at right, Fig. 9) was unprotected type 403 (modified) stainless steel. The shield, made of 1 mm (0.04 in.) thick rolled strip and brazed onto the leading edge, resisted erosion quite effectively, but the unprotected base metal did not.

Both blade portions shown in Fig. 9 also illustrate the dependence of erosion on hydrodynamic intensity. Damage was most severe at the leading edge, where hydrodynamic intensity was greatest. Away from the leading edge, impacting droplets were smaller, impact velocity was lower, and impact occurred at oblique rather than right angles; therefore, damage was progressively less severe.

It may be impossible to reduce the hydrodynamic intensity significantly without seriously degrading performance. In such instances, the use of erosion-resistant metals could be the only practical solution to a problem of liquid erosion. Many of the erosion-resistant metals can be applied as welded overlays; this makes salvage or repair of damaged surfaces easier or surface treatment of new components less costly than would be possible if the component had to be made entirely of erosion-resistant metal. Because liquid erosion is basically a surface phenomenon, the use of erosion-resistant overlays is effective in combating damage. Stellite alloys and stainless steels are the alloys most widely used as overlays.

However, many small parts are not amenable to protection by using erosion-resistant overlays. Therefore, the most effective means of combatting erosion of small parts is to increase the hardness of the metal or to specify a more erosion-resistant metal.

Erosion-Corrosion

When movement of a corrodent over a metal surface increases the rate of attack due to mechanical wear and corrosion, the attack is called erosion-corrosion. It is encountered when particles in a liquid impinge on a metal surface, causing the removal of protective surface films, such as air-formed protective oxide films and adherent corrosion products, and exposing new reactive surfaces, which are anodic to uneroded neighboring areas on the surface. This results in rapid localized corrosion of the exposed areas in the form of smooth-bottomed shallow recesses.

Nearly all flowing and turbulent corrosive media can cause erosion-corrosion. The attack can exhibit a directional pattern related to the path taken by the corrodent as it moves over the surface of the metal. Figure 10 shows the interior of a 50 mm (2 in.) copper river waterline that has suffered pitting and general erosion due to excessive velocity of the water. The brackish river water contained some suspended solids that caused the polishing of the copper pipe surface. The horseshoe-shaped pits (facing upstream) are typical of the damage caused by localized turbulence. The copper pipe was replaced with fiberglass-reinforced plastic piping.

In piping systems, erosion-corrosion can be reduced by increasing the diameter of the pipe, thus decreasing velocity and turbulence. Streamlining bends is useful in minimizing the effects of impingement. Inlet pipes should not be directed onto the vessel walls if it can be avoided. Flared tubing can be used to reduce problems at the inlet tubes in a tube bundle. Erosion-corrosion presents a distinct appearance. The metal surface usually exhibits severe weight loss, with many hollowed-out regions; the overall surface has a carved appearance along the pipe or tube wall.

Impingement attack or corrosion is a term used to describe some severe forms of erosion-corrosion, where impingement is encountered and erosion is more intense. It occurs frequently in turns or elbows of tubes and pipes and on surfaces of impellers and turbines. Figure 11 shows an example of this type of erosion-corrosion. The combined effects of high velocities and corrosion are clearly visible on the pump impeller. Impingement corrosion attack can also occur as the result of

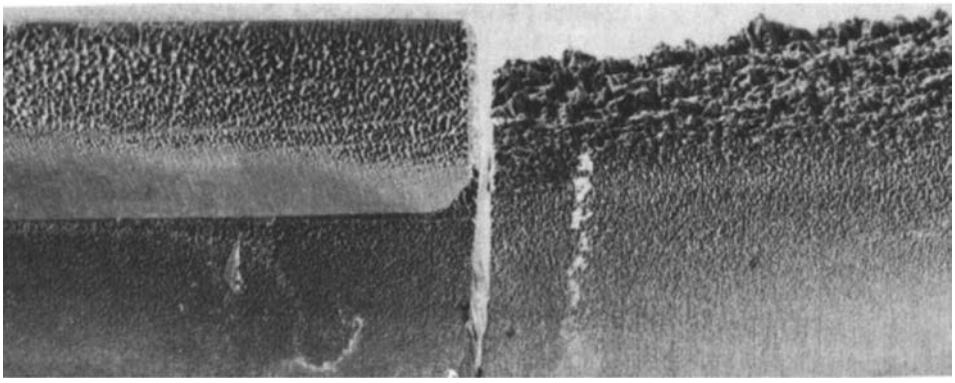

Fig. 9 Two portions of a modified type 403 stainless steel steam turbine blade damaged by liquid impingement erosion. The portion at left was protected by a 1 mm (0.04 in.) thick shield made of rolled Stellite 6B brazed onto the leading edge of the blade; the portion at right was unprotected. Note the difference in amounts of metal lost from protected and unprotected portions. Original magnification of both: 2.5×

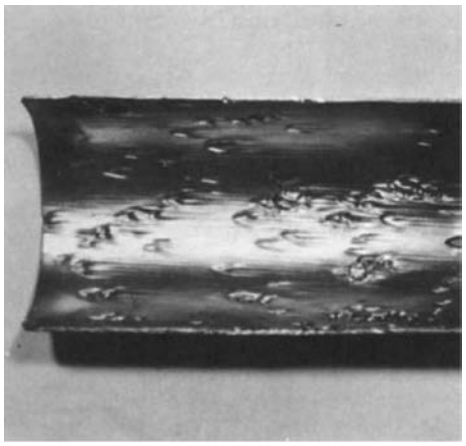

Fig. 10 Erosion pitting caused by turbulent river water flowing through copper pipe. The typical horseshoe-shaped pits point upstream. Original magnification: 0.5×

Fig. 11 Classic appearance of erosion-corrosion in a CF-8M (cast equivalent of wrought AISI 316 stainless steel) pump impeller

partial blockage of a tube. The impinging stream can rapidly perforate tube walls, especially if silt or mud has an additional erosive effect. Steam erosion is another form of impingement corrosion. It occurs when high-velocity wet steam contacts a metal surface. The resulting attack usually produces a roughened surface showing a large number of small cones with the points facing in the direction of flow.

Impingement attack often produces a horseshoe-shaped pit, where the deep undercut end points in the direction of flow. This form of attack frequently occurs in condenser systems handling seawater or brackish water that contains entrained air or solid particles and circulates through the system at relatively high velocities and with turbulent flow. The pits are elongated in the direction of flow and are undercut on the downstream side. When the condition becomes serious, a series of horseshoe-shaped grooves with the open ends on the downstream side can be formed. As the attack progresses, the pits can join one another, forming fairly large patches of undercut pits.

When impingement attack occurs in heat-exchanger and condenser tubing, it is usually confined to a short distance on the inlet end of the tube where the fluid flow is turbulent. Impingement attack can be controlled by use of corrosion-resistant alloys, such as 70%Cu-30%Ni alloy (UNS C71500). Impingement attack also has been somewhat relieved by inserting relatively short, tapered plastic and alloy sleeves inside the tube on the inlet end of the tube bundle. Other corrective measures include decreasing the velocity, streamlining the fluid flow, and decreasing the amount of entrained air or solid particles. These can be achieved by a streamlined design of water boxes, injector nozzles, and piping. Abrupt angular changes in the direction of fluid flow, low-pressure pockets, obstruction to smooth flow, and any other feature that can cause localized high velocities and turbulence of the circulating water should be minimized. Sacrificial impingement baffles can minimize damage to the shell-side surfaces of tubes.

Fig. 12 A 455 mm (18 in.) diameter cast iron suction bell from a low-pressure general service water pump that failed by cavitation erosion after approximately 5 years of service. Note the deeply pitted surface and irregular shape of the erosion pattern, both of which are typical characteristics of cavitation damage.

Cavitation Erosion

The most severe form of erosion-corrosion is cavitation erosion, although cavitation damage can occur without active corrosion. Cavitation principally occurs when relative motion between a metal surface and a liquid environment causes vapor bubbles to appear. When the bubbles collapse, they impose hammerlike blows simultaneously with the initiation of tearing action, which appears to pull away portions of the surface. Although the tearing action can remove any protective oxide film that exists on the surface of a metal, exposing active metal to the corrosive influence of the liquid environment, corrosion is not essential to cavitation erosion. When high velocities give rise to extremely low-pressure areas, as in a jet or rotary pump, vapor bubbles collapse at high-pressure areas and destroy the protective film on the metal surface or disrupt the metal itself.

Cavitation erosion occurs typically on rotors and pumps, on the trailing faces of propellers and of water turbine blades, and on the water-cooled side of diesel engine cylinders. Damage can be reduced by operating rotary pumps at the highest possible head of pressure to avoid formation of bubbles. For turbine blades, aeration of water serves to cushion the damage caused by the collapse of bubbles. Neoprene and similar elastomer coatings on metals are reasonably resistant to damage from this cause.

Cavitation erosion occurs in regions of a system where a combination of temperature and flow velocity causes growth and subsequent collapse of large quantities of vapor-filled bubbles in a flowing stream of liquid. Damage occurs at the points of bubble collapse. In steam plants, the components most often damaged by cavitation erosion are feed lines, pump casings, and pump impellers. Figure 12 shows the typical appearance of a part extensively damaged by cavitation erosion; the surface is deeply and irregularly pitted.

Cavitation erosion is most effectively avoided by reduction of either flow velocity or temperature (reduction of flow velocity is preferable). Other measures include selection of material and the use of erosion-resistant welded overlays.

Materials Selection for Applications in Which Erosive Wear Failures Can Occur

There is no universal material suitable for all types of erosive wear, especially when price is considered (Table 1). The effects of the indicated aspects are generalized and could sometimes differ from those indicated for some specific conditions. The metals (titanium, copper, etc.) and their alloys are not included due to their very specific areas of applications. In general, polymers have very low resistance against erosive wear and can be mainly used at lowest velocities (Ref 87). Elastomers usually have low erosion rates at low velocities and/or high impact angles. Ceramics are preferable for conditions where high erosion resistance is required and additional corrosive and oxidative effects occur. Ceramic-metal composites are more susceptible to these effects, while they perform better in dynamic conditions where impact is present and brittle fracturing can be an issue. Composites are usually more expensive than conventional materials, and their properties depend on content, arrangement, and properties of their constituents. If possible, lower velocities, more rounded particles, impact angles sufficiently higher or lower than the peak erosion angle, and noncorrosive liquids are preferred to reduce the erosive wear rate. Increasing temperature usually results in higher erosion rates, while increasing the ductility of ceramics or the formation of wear-resistant oxide layers could be beneficial.

Equations proposed in this article and computational simulations (Ref 93) should facilitate the analysis of erosive conditions and help to select the proper material and to

Table 1 Comparative properties and characteristics of various materials for service in erosive wear applications

Material	Price level (of the same volume of material)	Material behavior	Peak erosion angle	Maximum applicable velocity	Resistance to additional effect of corrosive liquid	Resistance to high-temperature erosion
Elastomers (e.g., rubbers)	2	Elastic	1	2–3	3–5	1–2
Unreinforced plastics	1–2	Ductile-brittle	1–4	1–2	3–5	1–2
Stainless steels and high-temperature alloys	4–5	Ductile	2	3	3–5	4–5
Steels	2	Ductile	2	3	1–2	1–2
Ceramic-metal composites (e.g., cermets)	5	Mixed	3–5	3–5	2–5	2–5
Technical ceramics	3–5	Brittle	4–5	3–5	4–5	2–5

Note: Rating range: 1, lowest; 5, highest

adjust working conditions to increase component service life. Laboratory and field testing of materials is strongly advised to support theoretical conclusions. Laboratory testing equipment settings should be adjusted to mimic as close as possible the conditions experienced in real application (Ref 94–97). The manner in which the particles or media approach the material surface (e.g., flux rate) influences the particle-particle and particle-surface interactions, mechanism, and rate of erosion. Possible rebounding of particles (especially during a normal angle of impact during gas-jet erosion testing) can cause shielding of the surface, changing the attack angle. The erodent particles and their fine fragments may be attached to the tribolayer even electrostatically, and their presence during following impacts can lead to an increase in local stresses (Ref 87, 93, 95, 96, 98, 99).

ACKNOWLEDGMENT

This article was revised from Thomas A. Adler, "Erosive Wear Failures," *Failure Analysis and Prevention*, Volume 11, *ASM Handbook*, ASM International, 2002, p 995–1001.

REFERENCES

1. "Standard Terminology Relating to Wear and Erosion," G 40, *Annual Book of ASTM Standards,* ASTM International
2. J. Stringer, Practical Experience with Wastage at Elevated Temperatures in Coal Combustion Systems, *Wear,* Vol 186–187, 1995, p 11–27
3. B.-E. Lee, C.A.J. Fletcher, and M. Behnia, Computational Study of Solid Particle Erosion for a Single Tube in Cross Flow, *Wear,* Vol 240, 2000, p 95–99
4. B.-E. Lee, C.A.J. Fletcher, and M. Behnia, Computational Prediction of Tube Erosion in Coal Fired Power Utility Boilers, *J. Eng. Gas Turbines Power (Trans. ASME),* Vol 121, Oct 1999, p 746–750
5. J.F. Drennen and J.G. McGowan, Prediction of Flyash Erosion in Convective Pass Sections of Coal Fired Systems, *Proc. Seventh Int. Conf. Erosion by Liquid and Solid Impacts,* University of Cambridge, 1987, p 75-1 to 75-6
6. J.J. Xie and P.M. Walsh, Erosion-Oxidation of Carbon Steel in the Convection Section of an Industrial Boiler Cofiring Coal-Water Fuel and Natural Gas, *J. Eng. Gas Turbines Power (Trans. ASME),* Vol 119, July 1997, p 717–722
7. M. Sucking and C. Allen, Critical Variables in High Temperature Erosive Wear, *Wear,* Vol 203–204, 1997, p 528–536
8. A. Levy, *Solid Particle Erosion and Erosion-Corrosion of Materials,* ASM International, 1995, p 7, 15, 62, 63, 98–102, 122–128
9. A.V. Levy, B.Q. Wang, G.Q. Geng, and W. Mack, Erosion-Corrosion of Steels in the Convection Pass Region of a Commercial Circulating Fluidized Bed Combustor, *Wear of Materials 1991,* American Society of Mechanical Engineers, 1991, p 697–701
10. A.V. Levy, B.Q. Wang, G.Q. Geng, and W. Mack, "*Erosivity of Particles in Circulating Fluidized Bed Combustors*," Paper 543, Corrosion '89, National Association of Corrosion Engineers, 1989
11. A. Levy and Y.-F. Man, Erosion-Corrosion of Chromium Steels, *Proc. Corrosion-Erosion-Wear of Materials at Elevated Temperatures, 1986,* National Association of Corrosion Engineers, 1987, p 168–203
12. A.V. Levy, B.-Q. Wang, Y.-F. Man, and N. Jee, Erosion-Corrosion of Steels in Simulated and Actual Fluidized Bed Combustor Environments, *Wear,* Vol 131, 1989, p 85–103
13. H.H. Krause and I.G. Wright, Boiler Tube Failures in Municipal Waste-to-Energy Plants, *Mater. Perform.,* Vol 35, Jan 1996, p 46–54
14. N.G. Solomon, Erosion-Resistant Coatings for Fluidized Bed Boilers, *Mater. Perform.,* Vol 37, 1998, p 38–43
15. P.M. Rogers, I.M. Hutchings, J.A. Little, and F. Kara, Microstructural Characterization of Surface Layers Formed on Alloy Steel during Erosion-Oxidation in a Fluidized Bed, *J. Mater. Sci.,* Vol 32, 1997, p 4575–4583
16. M.S. Crowley, Know Causes of, Solutions to, CFB-Boiler Refractory Problems, *Power,* Vol 136, Jan 1992, p 54–57
17. R.C. Tucker and A.A. Ashari, The Structure Property Relationship of Erosion Resistant Thermal Spray Coatings, *Proc. 15th Int. Thermal Spray Conf.,* ASM International, 1998, p 259–262
18. P.N. Walsh, J.M. Quets, and R.C. TuckerJr., Coatings for the Protection of Turbine Blades from Erosion, *J. Eng. Gas Turbines Power (Trans. ASME),* Vol 117, Jan 1995, p 152–155
19. I.A. Diaz-Tous, A.H. Khan, and T.H. McCloskey, Solid Particle Erosion Technology Assessment, *Advances in Steam Turbine Technology for the Power Generation Industry, PWR,* Vol 26, American Society of Mechanical Engineers, 1994, p 247–254
20. W. Tabakoff, M. Metwally, and A. Hamed, High-Temperature Coatings for Protection against Turbine Deterioration, *J. Eng. Gas Turbines Power (Trans. ASME),* Vol 117, Jan 1995, p 146–151
21. J.E. Restall and D.J. Stephenson, High Temperature Erosion of Coated Superalloys for Gas Turbines, *Mater. Sci. Eng.,* Vol 88, 1987, p 273–282
22. M. Menguturk and E.F. Sverdrup, Calculated Tolerance of a Large Electric Utility Gas Turbine to Erosion Damage by Coal Gas Ash Particles, *Erosion: Prevention and Useful Applications,* STP 664, American Society for Testing and Materials, 1979, p 193–224
23. S. Seetharamu, P. Sampathkumaran, and R.K. Kumar, Erosion Resistance of Permanent Moulded High Chromium Iron, *Wear,* Vol 186–187, 1995, p 159–167
24. C.R. Dimond, The Specification and Installation of Alumina Ceramics in Industry, *Mater. Des.,* Vol 8, May/June 1987, p 152–155
25. T.D. Johnson, M.B.J. Low, M.T. Parry, and D.J. Wall, Erosion in Pulverized Fuel Distribution Systems: Materials Selection and Plant Performance, *Proc. Seventh Int. Conf. Erosion by Liquid and Solid Impacts,* University of Cambridge, 1987, p 74-1 to 74-8
26. R.G. Wellman and C. Allen, The Effects of Angle of Impact and Materials Properties on the Erosion Rates of Ceramics, *Wear,* Vol 186–187, 1995, p 117–122
27. S.J. Dapkunas, A Summary of Erosion Experience in the U.S. Department of Energy's Coal Conversion Plants, *Proc. Fifth Int. Conf. Erosion by Liquid and Solid Impact,* University of Cambridge, 1979, p 43-1 to 43-14
28. S. Danyluk, W.J. Shack, J.Y. Park, and M. M. Mamoun, Solid Particle Erosion of a Cyclone from a Coal Gasification Pilot Plant, *Wear of Material 1981,* American Society of Mechanical Engineers, 1981, p 619–624
29. C.A. Youngdahl, K. Pater, and M.J. Gorski, Erosive Wear and Design Evaluation of a Stainless Steel Cyclone on the Gasification Pilot Plant Facility at Morgantown, *The Properties and Performance of Materials in the Coal Gasification Environment,* American Society for Metals, 1981, p 709–734
30. J.S. Hansen, Relative Erosion Resistance of Several Materials, *Erosion: Prevention and Useful Applications,* STP 664, American Society for Testing and Materials, 1979, p 148–162
31. J.S. Hansen, J.E. Kelly, and F.W. Wood, "*Erosion Testing of Potential Valve Materials for Coal Gasification Systems*," Report of Investigations 8335, U.S. Department of the Interior, Bureau of Mines, 1979
32. A. Drotlew, P. Christodoulou, and V. Gutowski, Erosion of Ferritic Fe-Cr-C Cast Alloys at Elevated Temperatures, *Wear,* Vol 211, 1997, p 120–128
33. R. Hamzah, D.J. Stephensen, and J.E. Strutt, Erosion of Material Used in Petroleum Production, *Wear,* Vol 186–187, 1995, p 493–496
34. L. Nøkleberg and T. Søntvedt, Erosion in Choke Valves—Oil and Gas Industry Applications, *Wear,* Vol 186–187, 1995, p 401–412
35. K. Haugen, O. Kvernvold, A. Ronold, and R. Sandberg, Sand Erosion of Wear-Resistant Materials: Erosion in Choke Valves, *Wear,* Vol 186–187, 1995, p 179–188

36. R.J.K. Wood and D.W. Wheeler, Design and Performance of a High Velocity Air-Sand Jet Impingement Erosion Facility, *Wear,* Vol 220, 1998, p 95–112
37. N. Gladys and V. Laura, Analysis of Rotor-Blade Failure due to High Temperature Corrosion/Erosion, *Surf. Coat. Technol.,* Vol 120–121, 1999, p 145–150
38. K.G. Budinski, Erosion of 316 Stainless Steel by Dicalcium Phosphate, *Wear,* Vol 186–187, 1995, p 145–149
39. E. Deaquino, D. Martínez, A. Perez, A. Velasco, M.A. Flores, and R. Viramontes, *Powder Technol.,* Vol 95, 1998, p 55–60
40. D.A. Brosnan, M.S. Crowley, and R.C. Johnson, CPI Drive Refractory Advances, *Chem. Eng.,* Vol 105, Oct 1998, p 110–120
41. G.P. Tilly, Sand Erosion of Metals and Plastics: A Brief Review, *Wear,* Vol 14, 1969, p 241–248
42. R.W. Bruce, Development of 1232 °C (2250 °F) Erosion and Impact Tests for Thermal Barrier Coatings, *Tribol. Trans.,* Vol 41, 1998, p 399–410
43. C.E. Smeltzer, M.E. Gulden, and W.A. Compton, Mechanism of Metal Removal by Impacting Dust Particles, *J. Basic Eng. (Trans. ASME*), Vol 92, Sept 1970, p 639–654
44. F. Wiesinger, F. Sutter, F. Wolfertstetter, N. Hanrieder, A. Fernández-García, R. Pitz-Paal, and M. Schmücker, Assessment of the Erosion Risk of Sandstorms on Solar Energy Technology at Two Sites in Morocco, *Sol. Energy,* Vol 162, 2018, p 217–228
45. R. Chattopadhyay, *Green Tribology, Green Surface Engineering, and Global Warming,* ASM International, 2014
46. A. Kumar Rai, A. Kumar, and T. Staubli, Effect of Concentration and Size of Sediments on Hydro-Abrasive Erosion of Pelton Turbine, *Renew. Energy,* Vol 145, 2020, p 893–902
47. J.A. Hawk, R.D. Wilson, D.R. Danks, and M.T. Kiser, Abrasive Wear Failures, *Failure Analysis and Prevention,* Vol 11, *ASM Handbook,* ASM International, 2002
48. K.H. Zum Gahr, Microstructure and Wear of Materials, *Tribology Series,* Vol 10, Elsevier Amsterdam, 1987
49. I. Hussainova, Some Aspects of Solid Particle Erosion of Cermets, *Tribol. Int.,* Vol 34, 2001, p 89–93
50. J.G.A. Bitter, A Study of Erosion Phenomena, Parts I and II, *Wear,* Vol 6, 1963, p 5–21, 169–190
51. A.K. Cousens and I.M. Hutchings, Influence of Erodent Shape on the Erosion of Mild Steel, *Proc. Sixth Int. Conf. Erosion by Liquid and Solid Impact,* University of Cambridge, 1983, p 41-1 to 41-8
52. G. Sundararajan, A Comprehensive Model for the Solid Particle Erosion of Ductile Materials, *Wear of Materials 1991,* American Society of Mechanical Engineers, 1991, p 503–511
53. M. Roy, Y. Tirupatataiah, and G. Sundararajan, Effect of Particle Shape on the Erosion of Cu and Its Alloys, *Mater. Sci. Eng. A,* Vol 165, 1993, p 51–63
54. P.V. Rao and D.H. Buckley, Time Effects of Erosion by Solid Particle Impingement on Ductile Materials, *Proc. Sixth Int. Conf. Erosion by Liquid and Solid Impact,* University of Cambridge, 1983, p 38-1 to 38-10
55. M. Antonov and I. Hussainova, Cermets Surface Transformation under Erosive and Abrasive Wear, *Tribol. Int.,* Vol 43, 2010, p 1566–1575
56. I. Finnie, The Mechanism of Erosion of Ductile Metals, *Proc. Third U.S. National Congress of Applied Mechanics,* American Society of Mechanical Engineers, 1958, p 527–532
57. I. Finnie, Erosion of Surfaces by Solid Particles, *Wear,* Vol 3, 1960, p 87–103
58. I. Finnie, Erosion by Solid Particles in a Fluid Stream, *Symposium on Erosion and Cavitation,* STP 307, American Society for Testing and Materials, 1962, p 70–82
59. J.H. Neilson and A. Gilchrist, Erosion by a Stream of Solid Particles, *Wear,* Vol 11, 1968, p 111–122
60. R.E. Winter and I.M. Hutchings, Solid Particle Erosion Studies Using Single Angular Particles, *Wear,* Vol 29, 1974, p 181–194
61. G.P. Tilly, A Two Stage Mechanism of Ductile Erosion, *Wear,* Vol 23, 1973, p 87–96
62. S.M. Wiederhorn and B.J. Hockey, Effect of Material Parameters on the Erosion Resistance of Brittle Materials, *J. Mater. Sci.,* Vol 18, 1983, p 766–780
63. A.W. Ruff and S.M. Wiederhorn, Erosion by Solid Particle Impact, *Treatise on Material Science and Technology,* Vol 16, Academic Press, 1979, p 69–126
64. A.G. Evans, M.E. Gulden, and M. Rosenblatt, Impact Damage in Brittle Materials in the Elastic-Plastic Response Regime, *Proc. R. Soc. (London) A,* Vol 361, 1978, p 343–365
65. R. BellmanJr. and A. Levy, Erosion Mechanism in Ductile Metals, *Wear,* Vol 70, 1981, p 1–27
66. A.V. Levy, The Platelet Mechanism of Erosion of Ductile Metals, *Wear,* Vol 108, 1986, p 1–21
67. I.M. Hutchings, A Model for the Erosion of Metals by Spherical Particles at Normal Incidence, *Wear,* Vol 70, 1981, p 269–281
68. P.S. Follansbee, G.B. Sinclair, and J.C. Williams, Modelling of Low Velocity Particulate Erosion in Ductile Materials by Spherical Particles, *Wear,* Vol 74, 1982, p 107–122
69. A.V. Levy and S. Jahanmir, *The Effects of the Microstructure of Ductile Alloys on Solid Particle Erosion Behavior*, *Corrosion-Erosion Behavior of Materials,* TMS-AIME, 1980, p 177–189
70. S. Jahanmir, The Mechanics of Subsurface Damage in Solid Particle Erosion, *Wear,* Vol 61, 1980, p 309–324
71. T. Christman and P.G. Shewmon, Adiabatic Shear Localization and Erosion of Strong Aluminum Alloys, *Wear,* Vol 54, 1979, p 145–155
72. G. Sundararajan and P.G. Shewmon, A New Model for the Erosion of Metals at Normal Incidence, *Wear,* Vol 84, 1983, p 237–258
73. M. Parsi, K. Najmi, F. Najafifard, S. Hassani, B.S. McLaury, and S.A. Shirazi, A Comprehensive Review of Solid Particle Erosion Modeling for Oil and Gas Wells and Pipelines Applications, *J. Nat. Gas Sci. Eng.,* Vol 21, 2014, p 850–873, http://dx.doi.org/10.1016/j.jngse.2014.10.001
74. M. Stack, B.D. Jana, and S.M. Abdelrahman, Models and Mechanisms of Erosion-Corrosion in Metals, *Tribocorrosion of Passive Metals and Coatings,* Woodhead Publishing Ltd., Cambridge, U.K., 2011, ISBN 9781845699666
75. I.M. Hutchings, Mechanical and Metallurgical Aspects of the Erosion of Metals, *Proc. Corrosion/Erosion of Coal Conversion Systems Materials Conf.,* National Association of Corrosion Engineers, 1979, p 393–428
76. P.H. Shipway and I.M. Hutchings, The Role of Particle Properties in the Erosion of Brittle Materials, *Wear,* Vol 193, 1996, p 105–113
77. G. Sundararajan and M. Roy, Solid Particle Erosion Behavior of Metallic Materials at Room and Elevated Temperatures, *Tribol. Int.,* Vol 30, 1997, p 339–359
78. I.M. Hutchings, Mechanisms of the Erosion of Metals by Solid Particles, *Erosion: Prevention and Useful Applications,* STP 664, American Society for Testing and Materials, 1979, p 59–76
79. I. Finnie, A. Levy, and D.H. McFadden, Fundamental Mechanisms of the Erosive Wear of Ductile Metals by Solid Particles, *Erosion: Prevention and Useful Applications,* STP 664, American Society for Testing and Materials, 1979, p 36–58
80. S. Bahadur and R. Badruddin, Erodent Particle Characterization and the Effect of Particle Size and Shape on Erosion, *Wear of Materials 1989,* Vol 1, American Society of Mechanical Engineers, 1989, p 143–153
81. A.V. Levy and P. Chik, The Effects of Erodent Composition and Shape on the Erosion of Steel, *Wear,* Vol 89, 1983, p 151–162
82. I. Kleis, Probleme der Bestimmung des Strahlverschleisses bei Metallen (The Problem of the Determination of the Wear of Metals by a Beam (of Abrasive Particles)), *Wear,* Vol 13, 1969, p 199–215
83. A. Magnée, Generalized Law of Erosion: Application to Various Alloys and

Intermetallics, *Wear,* Vol 181–183, 1995, p 500–510
84. A. Mishra and I. Finnie, On the Size Effect in Abrasive and Erosive Wear, *Wear,* Vol 65, 1981, p 359–373
85. J.R. Nicholls, Laboratory Studies of Erosion-Corrosion Processes under Oxidizing and Oxidizing/Sulphidising Conditions, *Mater. High Temp.,* Vol 14, 1997, p 289–306
86. J.C Arnold and I.M. Hutchings, The Erosive Wear of Elastomers, *J. Nat. Rubber Res.,* Vol 6 (No. 4), 1991, p 241–256
87. M. Antonov, J. Pirso, D. Goljandin, A. Vallikivi, and I. Hussainova, Effect of Fine Erodent Retained on the Surface during Erosion of Metals, Ceramics, Plastic, Rubber and Hardmetal, *Wear,* Vol 354–355, 2016, p 53−68, 10.1016/j.wear.2016.02.018
88. Y. Xie, J. Jiang, and M.A. Islam, Elastomers and Plastics for Resisting Erosion Attack of Abrasive/Erosive Slurries, *Wear,* Vol 426–427, 2019, p 612–619
89. N. Ojala, K. Valtonen, J. Minkkinen, and V. T. Kuokkala, Edge and Particle Embedment Effects in Low- and High-Stress Slurry Erosion Wear of Steels and Elastomers, *Wear,* Vol 388–389, 2017, p 126–135
90. I. Finnie, Some Observations on the Erosion of Ductile Metals, *Wear,* Vol 19, 1972, p 81–90
91. A. Ots, *Oil Shale Fuel Combustion,* Tallinna Raamatutrükikoda, 2006, ISBN 9789949137101
92. Y. Yonemoto and T. Kunugi, Analytical Consideration of Liquid Droplet Impingement on Solid Surfaces, *Sci. Rep.,* Vol 7 (No. 1), 2017, p 2362
93. V.B. Nguyen, Q.B. Nguyen, C.Y.H. Lim, Y. W. Zhang, and B.C. Khoo, Effect of Air-Borne Particle-Particle Interaction on Materials Erosion, *Wear,* Vol 322–323, 2015, p 17–31
94. M.G. Gee and I.M. Hutchings, "*General Approach and Procedures for Erosive Wear Testing*," Measurement Good Practice Guide 56, National Physical Laboratory, ISSN 1368–6550
95. T. Deng, M.S. Bingley, M.S. Bradley, and S.R. De Silva, A Comparison of the Gas-blast and Centrifugal-Accelerator Erosion Testers: The Influence of Particle Dynamics, *Wear,* Vol 265 (No. 7–8), 2008, p 945–955
96. V. Javaheri, D. Porter, and V.-T. Kuokkala, Slurry Erosion of Steel—Review of Tests, Mechanisms and Materials, *Wear,* Vol 408–409, 2018, p 248–273, doi:10.1016/j.wear.2018.05.010
97. M. Antonov, D.-L. Yung, D. Goljandin, V. Mikli, and I. Hussainova, Effect of Erodent Particle Impact Energy on Wear of Cemented Carbides, *Wear,* Vol 376–377, 2017, p 507–515, http://dx.doi.org/10.1016/j.wear.2016.11.032
98. M. Varga, M. Antonov, M. Tumma, K. Adam, and K.O. Alessio, Solid Particle Erosion of Refractories: A Critical Discussion of Two Test Standards, *Wear,* Vol 426–427, 2019, p 552–561
99. I. Kleis and P. Kulu, *Solid Particle Erosion: Occurrence, Prediction and Control,* Springer-Verlag London, 2008, ISBN 978-1-84800-028-5